Investigating dopant diffusion enhancement at grain boundaries in multicrystalline silicon wafers with micro-photoluminescence spectroscopy

Hieu T. Nguyen, Sudha Mokkapati, and Daniel Macdonald

Employing micro-photoluminescence spectroscopy at low temperatures, we are able to detect dopant diffusion enhancement along various grain boundaries and sub-grain boundaries in multicrystalline silicon wafers. We find an enhancement of phosphorus diffusion not only at all investigated grain boundary types, including Σ3, Σ5, Σ9, Σ11, Σ27a, and random large angle, but also at sub-grain boundaries. In addition, the sub-grain boundaries are demonstrated to contain a high density of defects and impurities distributed uniformly depth-wise across the wafer thickness, suggesting that the presence of defects and impurities does not hinder the preferential diffusion of dopant atoms along the sub-grain boundaries. The results are validated with secondary electron dopant contrast images, which confirm the higher dopant concentration along the grain boundaries and sub-grain boundaries.

I. Introduction

Homogenous diffused junctions are important for high efficiency multicrystalline silicon (mc-Si) solar cells. However, diffusivities of dopant atoms along certain grain boundaries (GBs) are reported to be higher than in the intra-grain regions, thus creating deeper p-n junctions at these GBs [1,2]. This diffusion enhancement has been empirically studied using electron beam induced current (EBIC) [1] and light beam induced current (LBIC) [3] techniques. However, these techniques require not only contact formation to extract the induced current, but also an angle-lapping [1] or cross-sectioning [3] of the GBs to expose the junctions. Furthermore, there has been no experimental assessment of the diffusion enhancement along sub-grain boundaries (sub-GBs). Since sub-GBs often contain high densities of defects and impurities, they are very recombination active. Therefore, investigating the diffusion enhancement along the sub-GBs using EBIC and LBIC is limited because the defects/impurities and diffused dopants have opposing impacts on the induced current.

Recently, employing a micro photoluminescence spectroscopy (μ-PLS) system, we demonstrated the separation of luminescence peaks from diffused layers and the underlying silicon substrate at low temperatures [4,5], courtesy of band gap narrowing effects in heavily-doped silicon [6,7]. Furthermore, by varying the excitation wavelength, the penetration depth of the laser light inside silicon wafers can be controlled, and thus the depth distributions of different structures underneath the wafer surface can be assessed qualitatively [8]. In this work, we apply the technique to study the diffusion enhancement of dopant atoms along large angle GBs and sub-GBs. First, we demonstrate that the diffusion is enhanced for numerous types of large angle GBs, rather than only at some specific GBs as reported in the literature [3,9]. After that, we show that sub-GBs also enhance the dopant diffusion, even though they are decorated with a high density of defects and impurities. Our conclusions are supported by secondary electron (SE) images, which confirm the enhanced diffusion along both large angle GBs and sub-GBs. These results highlight the value of this nondestructive, contactless characterization technique in silicon photovoltaics.

II. Experimental details

The two investigated samples are standard boron-doped p-type mc-Si wafers with a boron doping of about 9×10^{15} cm^{-3}. They were cut from the two consecutive sister wafers from the same ingot. Both of them were chemically etched in HF/HNO_3 solution to remove saw damage and to achieve polished surfaces, and were then

immersed in a defect etchant consisting of HF/HNO_3/acetic acid for 16 hours to delineate the sub-grain boundaries [10,11]. One sample was kept at the as-cut state (after the defect etching step). The other sample went through a $POCl_3$ diffusion process at 850 ^oC for 1 hour, and then annealed in N_2 gas at 850 ^oC for another 1 hour. The resultant sheet resistance was measured on a controlled float-zone p-type wafer, and was found to be 10.5 Ω/□. The diffused sample was then immersed in HF to remove the phosphosilicate glass.

The setup of the μ-PLS system used here is described in detail in Ref. 6. An excitation light source with a tunable wavelength range from 490 nm to 2 μm was employed and focused onto the sample surface through confocal optics. In this work, a wavelength range of 510 – 810 nm with a bandwidth of 10 nm was used. Therefore, the on-sample illuminated spot size varied from 1 μm (for 510-nm excitation wavelength) to ~2 μm (for 810-nm excitation wavelength). The on-sample excitation power was kept constant at 6 mW for all excitation wavelengths. The spectral response of the entire system was determined with a calibrated halogen-tungsten lamp. The cross-sectional surfaces for scanning electron microscope (SEM) analysis were prepared with the focus ion beam (FIB) technique. GB types were determined from electron backscatter diffraction (EBSD) measurements.

III. Enhanced diffusion at large angle GBs

First, we demonstrate that there are more dopant atoms diffused along GBs than intra-grain regions. Figure 1a compares the normalized PL spectrum captured at 79K at a random large angle GB (black curve) with that captured at 15 μm away from the same GB (dashed-red curve) of the diffused mc-Si wafer, excited with the 510-nm wavelength. The spectrum at the same GB but from the as-cut wafer is also shown for comparison (dotted-blue curve). The main peak located at ~1130 nm is the band-to-band (BB) emission from the underlying Si substrate. The shoulder located at ~1160 nm is the band-to-band emission from the heavily-doped layer [4], denoted as HDBB peak (Heavily-Doped Band-to-Band). The HDBB peak captured at the GB is higher than that captured at 15 μm away, suggesting that the GB is more heavily doped than the surrounding regions. The peak around 1200 nm in the spectrum from the as-cut wafer is the phonon-replica of the BB peak, denoted as PRBB (Phonon-Replica of Band-to-Band).

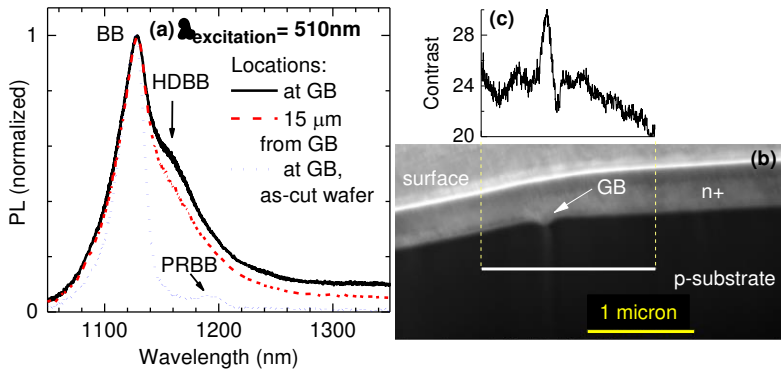

Figure 1: (a) Normalized PL spectra at a random large angle GB (black line) and 15 microns (dashed-red line) away from it of the diffused mc-Si wafer, excited with the 510-nm wavelength at 79 K. The grain misorientation is 53.4^0 around the [0 1 1] axis. The spectrum at the same GB from the as-cut mc-Si wafer (dotted-blue line) is also included for comparison. (b) Vertical cross-sectional SEM image of the investigated GB of the diffused mc-Si wafer. (c) SE contrast profile of the line scan marked with the white line in Figure 1b.

Figure 1b shows an SEM image of the vertical cross-section of the investigated GB. We can observe clearly the contrast difference between the n+ diffused layer and the p-type substrate. Compared to the common SEM contrast between n- and p-type Si (brighter for p-type and darker for n-type), the contrast in Figure 1b is inverted (brighter for n+ layer and darker for p-substrate) since the cross-sectional surface was contaminated with Ga atoms (whose work function is smaller than that of Si) during the FIB preparation. The mechanism of this contrast inversion was explained in detail in Ref. 12. The contrast profile scan in Figure 1c shows that, at the line scan position (about 1 µm below the surface) there are still considerable phosphorus atoms at the GB, i.e. the p-n junction extends much more deeply into the substrate at the GB than the adjacent regions.

Moreover, Figure 2 (a-d) compares the absolute PL spectra captured at the GB with those captured at 15 µm away from it of the diffused mc-Si wafer, with different excitation wavelengths at 79 K. In Figure 2a, the HDBB intensity is clearly higher at the GB than 15 µm away from it, although the BB intensity is the same. When the excitation wavelength increases (Figures 2b-d), both the BB peaks increase significantly in magnitude, as the impact of the surface recombination in the diffused layer is reduced and a larger fraction of the excitation light is absorbed in the bulk. The difference between the two HDBB shoulders is also reduced, consistent with the reduced absorption in the heavily-doped layer. Note that, in the spectrum from the as-cut wafer at 79 K (dotted-blue line in Figure 1a), the PL intensity around 1160 nm is only about 6% of the BB intensity. Therefore, the difference between the two HDBB peaks in Figure 2 is not due to the small difference between the two BB peaks.

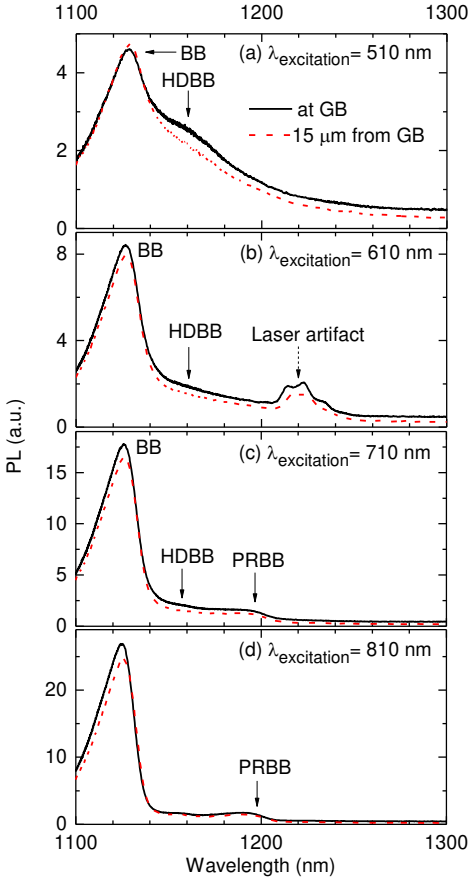

Figure 2: Comparison of absolute PL spectra at the random large angle GB (black line) and 15 microns (dashed-red line) away from it of the diffused mc-Si wafer, excited with different excitation wavelengths at 79 K. The spurious peak marked by the broken arrow in Figure 2b is an artifact from the laser. Its center wavelength is always twice of the excitation wavelength.

We captured the spectra from numerous large angle GBs including Σ3, Σ5, Σ9, Σ11, Σ27a, and random angle GBs, and always found an enhanced diffusion along these GBs. The results disagree with the findings reported in Ref. 3, in which the diffusion was shown to be enhanced along Σ3 GBs, but no enhanced diffusion was observed along Σ27a and random large angle GBs. Therefore, a detailed study on the diffusion mechanism of dopant atoms along different types of GBs under various conditions is required to clarify these uncertainties, and this contactless and non-destructive PLS-based method could be a powerful tool to study this diffusion mechanism without complex sample preparation.

IV. Enhanced diffusion at sub-GBs

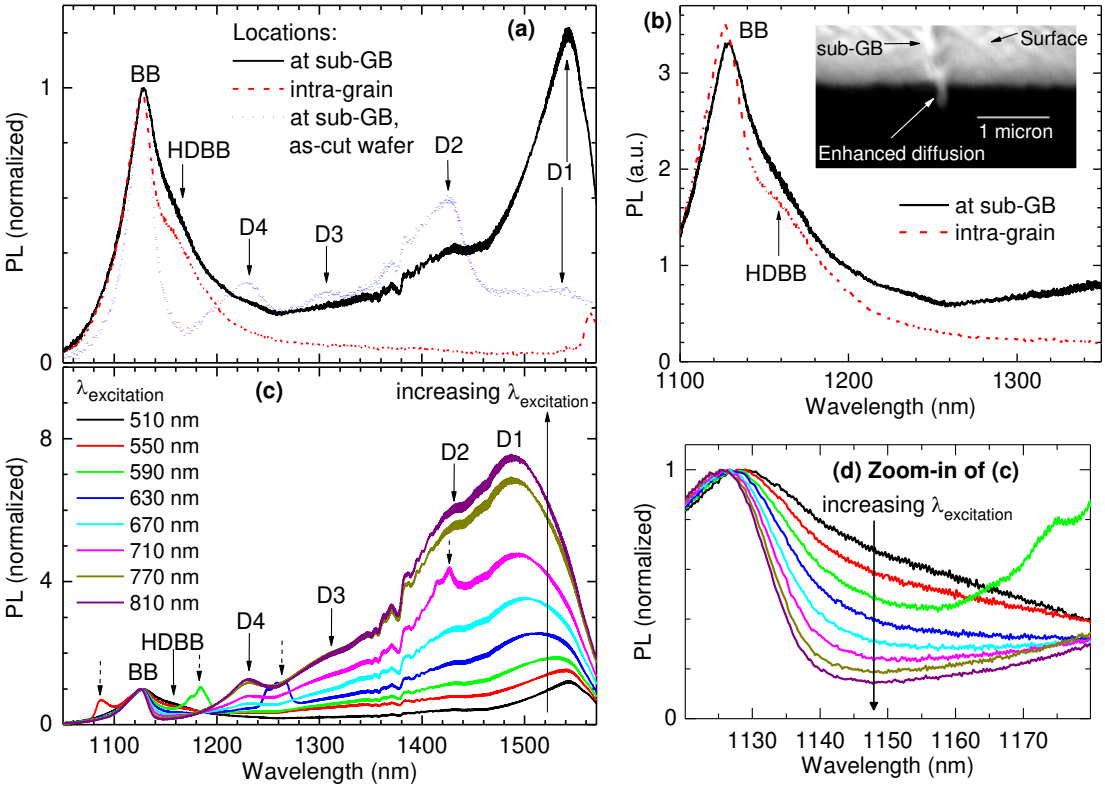

Figure 3: (a) Normalized and (b) absolute PL spectra at the sub-GB (black line) and the intra-grain region (dashed-red line) of the diffused mc-Si wafer, excited with the 510-nm wavelength. The spectrum at the same sub-GB from the as-cut mc-Si wafer (dotted-blue line) was also included for comparison. The insert in Figure 3b is a vertical cross-sectional SEM image of this sub-GB of the diffused mc-Si wafer. (c) Normalized PL spectra at the sub-GB of the diffused mc-Si wafer with different excitation wavelengths. (d) A zoom-in between 1120 and 1180 nm of Figure 3c. All measurements were done at 79 K. The normalized spectra were normalized to the band-to-band peak. The spurious peaks marked by broken arrows in Figure 3c are artifacts from the laser light.

Now, we investigate the distribution of dopant atoms around sub-GBs in mc-Si wafers after the phosphorus diffusion step. Sub-GBs contain a high density of dislocations due to the high thermal stress and strain during the ingot growing and cooling. Also, they are often decorated with secondary defects and impurities trapped by the dislocation networks. The dislocations themselves are known to emit two distinct deep-level PL peaks (the so-called D3 and D4 lines), whereas the surrounding secondary defects and impurities emit another two deep-level peaks (D1 and D2 lines) [13-16]. First, we examine sub-GBs at which the density of decorating defects and impurities is high. A typical PL spectrum at this kind of sub-GBs from the as-cut mc-Si wafer is given in

Figure 3a (dotted-blue curve). Besides the D3 and D4 peaks emitted from dislocations, the sub-GB also emits the D1 and D2 peaks due to decorating defects and impurities. Figures 3a and 3b compare the normalized and absolute PL spectra, respectively, of the diffused mc-Si wafer at 79 K, captured at the same sub-GB (black line) and the intra-grain region (dashed-red line). The intensity (both in normalized and absolute scales) of the HDBB peak at the sub-GB is higher than that at the intra-grain region, although the absolute BB intensity at the sub-GB is lower than that at the intra-grain region. The results suggest that there are more active dopant atoms along the sub-GB than the intra-grain regions. The dopant atoms are still preferentially diffused into the sub-GB even though there is a high density of defects and impurities around it. We note that although the D4 luminescence peak does partly overlap with the HDBB shoulder, making the comparison with the spectra measured away from the sub-GB more difficult, in this case the magnitude of the D4 luminescence is small enough to still conclude that there is an increased dopant concentration at the sub-GB. To fortify this conclusion, an SEM dopant contrast image was captured on a vertical cross-section of this sub-GB of the diffused wafer and is displayed as an insert in Figure 3b. The p-n junction clearly extends more deeply into the substrate at the sub-GB than the surrounding regions.

In addition, Figures 3c and 3d (a zoom-in of Figure 3c) show the evolution of normalized PL spectra with increasing excitation wavelengths, captured at the sub-GB of the diffused wafer at 79 K. In Figure 3c, the longer the excitation wavelength, the higher the intensities of the D lines. The results confirm that the defects (both intrinsic dislocations and secondary defects) and impurities are distributed depth-wise across the wafer thickness, rather than being limited to the near-surface region. In contrast, in Figure 3d, the shoulder around 1160 nm, attributed to the HDBB peak, is reduced significantly with increasing excitation wavelengths. This is because the HDBB peak is emitted from the diffused layer located near the surface.

Furthermore, we continue investigating sub-GBs which contain dislocations but a relatively low density of secondary defects and impurities, and thus emitting strong D3 and D4 but minimal D1 and D2 lines. Figures 4a and 4b compare the normalized PL spectra captured at a sub-GB (black curve) and 15 µm away from it (dashed-red curve) of the diffused mc-Si wafer at 79 and 300 K, respectively. The spectra at the same sub-GB but from the as-cut wafer are also presented for comparison. In Figure 4a, due to the intense D4 line, it is not possible to observe the HDBB shoulder at low temperatures. However, since the D3 and D4 lines display a strong thermal quenching rate [17], at room temperature these 2 lines are quenched significantly and the contribution of the HDBB peak into the total spectra is more obvious, as depicted in Figure 4b. As can be clearly seen from Figure 4b, around 1170 nm, the spectra from the as-cut wafer at and away from the sub-GB are not affected by the deep-level peaks. Nevertheless, the shoulder around 1170 nm (due to the HDBB peak) of the spectrum captured at the sub-GB (of the diffused wafer) is still broader than that captured at the intra-grain region. The results suggest that more dopants have diffused into this sub-GB than the surrounding regions. Note that, the carrier profile and surface reflectivity have a negligible impact on the PL spectral shape at the long wavelength side since reabsorption of the generated photons is negligible at these wavelengths, as demonstrated in Ref. 18.

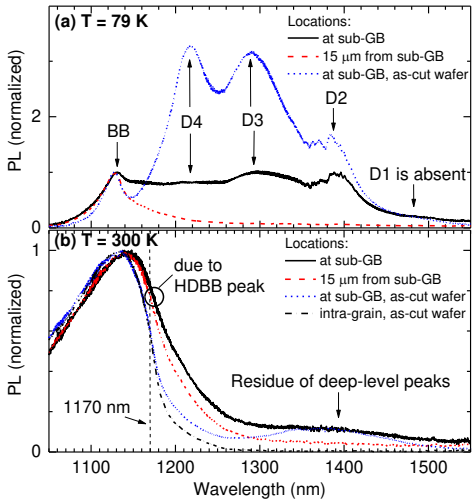

Figure 4: Normalized PL spectra at another sub-GB (black line) and 15 microns (dashed-red line) away from it of the diffused mc-Si wafer at (a) 79 K and (b) 300 K, excited with the 510-nm wavelength. The spectra at the same sub-GB (dotted-blue lines) and the intra-grain region (dashed-dotted black line) from the as-cut mc-Si wafer were also included for comparisons. The dashed-vertical line in Figure 4b is the location from which the intensity mapping in Figure 5b is extracted. The normalized spectra were normalized to the band-to-band peak.

Finally, Figures 5a shows a mapping of the total absolute PL intensity between 1000 and 1250 nm (the impact of the deep-level peaks is minimal in this range), whereas Figure 5b shows a mapping of the normalized PL intensity at 1170 nm, at room temperature around a sub-GB of the diffused mc-Si wafer. The dark line in Figure 5a indicates an increased recombination activity along the sub-GB due to the defects and impurities, whereas the bright line in Figure 5b indicates more dopant atoms diffused along this sub-GB since the broader long-wavelength shoulder is caused by the HDBB peak (see Figure 4b). The results from these two images confirm that, although the recombination activity is increased along the sub-GBs, more dopant atoms are also diffused into the sub-GBs. This conclusion could not be made based on EBIC or LBIC measurements since the total induced current is determined by both the defect/impurity and dopant concentrations. The defects and impurities reduce the current whereas the dopants increase it.

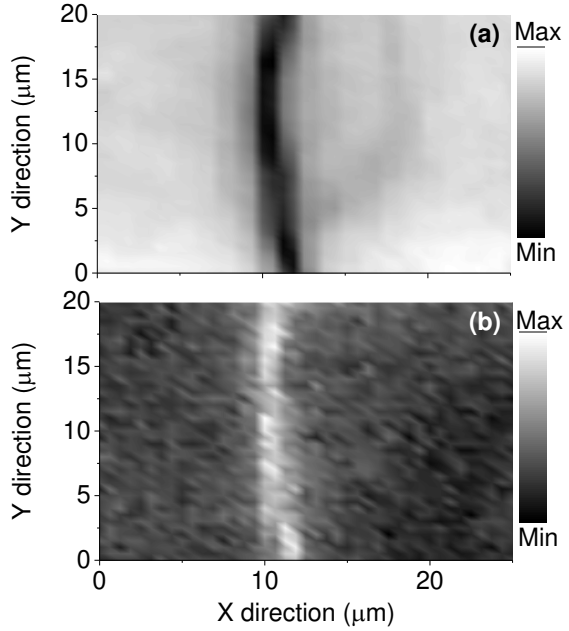

Figure 5: (a) Mapping of absolute PL intensity around a sub-GB of the diffused mc-Si wafer at 300 K. The intensity is the sum of the PL signal from 1000 to 1250 nm. (b) Mapping of normalized PL intensity at 1170-nm wavelength of the same area as Figure 5a at 300 K. The scanning step sizes are 0.5 µm in both x and y directions. The excitation wavelength is 532 nm.

V. Summary

In conclusion, applying the micro-photoluminescence spectroscopy techniques, we have detected the dopant diffusion enhancement along grain boundaries and sub-grain boundaries in multicrystalline silicon wafers. We have demonstrated that this enhancement happens at numerous types of grain boundaries, rather than only at some specific grain boundaries as reported in the literature. In addition, we have shown that the presence of defects and impurities around sub-grain boundaries does not hinder the preferential diffusion of dopant atoms. These findings help to demonstrate the value of such spectrally-resolved PL techniques in silicon photovoltaics.

Acknowledgement

This work has been supported by the Australian Research Council (ARC) and the Australian Renewable Energy Agency (ARENA) through research grant RND009. The Australian National Fabrication Facility is acknowledged for providing access to some of the facilities used in this work. The authors are in debt to Prof. H. Tan for providing access to the spectroscopic equipment, T. Duong and Dr. S. P. Phang for assisting with the sample preparation, and Dr. H. C. Sio for helping with the EBSD measurements.

[1] A.D. Buonaquisti, W. Carter, and P.H. Holloway, "Diffusion characteristics of boron and phosphorus in polycrystalline silicon," Thin Solid Films 100, 235 (1983)
[2] Y. Mishin and Chr. Herzig, "Grain boundary diffusion: recent progress and future research," Materials Science and Engineering A 260, 55 (1999).
[3] M. Breitwieser, F. D. Heinz, A. Büchler, M. Kasemann, J. Schön, W. Warta, and M. C. Schubert, "Analysis of solar cell cross sections with micro-light beam induced current (µLBIC)," Solar Energy Materials & Solar Cells 131, 124 (2014).
[4] H. T. Nguyen, D. Yan, F. Wang, P. Zheng, Y. Han, and D. Macdonald, "Micro-photoluminescence spectroscopy on heavily-doped layers of silicon solar cells," Physica Status Solidi RRL 9, 230 (2015).
[5] H. T. Nguyen, F. E. Rougieux, D. Yan, Y. Wan, S. Mokkapati, S. M. de Nicolas, J. P. Seif, S. De Wolf, and D. Macdonald, "Characterizing amorphous silicon, silicon nitride, and diffused layers in crystalline silicon solar cells using micro-photoluminescence spectroscopy," Solar Energy Materials & Solar Cells 145, 403 (2016).
[6] J. Wagner, "Photoluminescence and excitation spectroscopy in heavily doped n- and p-type silicon," Phys. Rev. B, vol. 29, pp. 2002-2009, 1984.
[7] J. Wagner, "Band-gap narrowing in heavily doped silicon at 20 and 300 K studied by photoluminescence," Phys. Rev. B, vol. 32, pp. 1323-1325, 1985.
[8] H. T. Nguyen, S. P. Phang, J. Wong-Leung, and D. Macdonald, "Photoluminescence excitation spectroscopy of diffused layers on crystalline silicon wafers," IEEE Journal of Photovoltaics 6, 746 (2016).
[9] H. J. Möller, Semiconductors for Solar Cells, Artech House, Boston, 1993.
[10] W.C. Dash, "Copper precipitation on dislocations in silicon," J. Appl. Phys 27, 1193 (1956).
[11] Y. Kashigawa, R. Shimokawa, and M. Yamanaka, "Highly sensitive etchants for delineation of defects in single- and polycrystalline silicon materials," J. Electrochem. Soc. 143, 4079 (1996).
[12] M. El-Gomati, F. Zaggout, H. Jayacody, S. Tear, and K. Wilson, "Why is it possible to detect doped regions of semiconductors in low voltage SEM: a review and update," Surface and Interface Analysis 37, 901 (2005).
[13] M. Tajima, Y. Iwata, F. Okayama, H. Toyota, H. Onodera, and T. Sekiguchi, "Deep-level photoluminescence due to dislocations and oxygen precipitates in multicrystalline Si," J. Appl. Phys., vol. 111, pp. 113523-1 - 113523-6, 2012.
[14] M. Tajima, "Spectroscopy and topography of deep-level luminescence in photovoltaic silicon," IEEE Journal of Photovoltatics, vol. 4, pp. 1452-1458, 2014.
[15] H. T. Nguyen, F. E. Rougieux, F. Wang, H. Tan, and D. Macdonald, "Micrometer-scale deep-level spectral photoluminescence from dislocations in multicrystalline silicon," IEEE Journal of Photovoltaics, vol. 5, pp. 799-804, 2015.
[16] H. T. Nguyen, F. E. Rougieux, F. Wang, and D. Macdonald, "Effects of solar cell processing steps on dislocation luminescence in multicrystalline silicon," Energy Procedia, vol. 77, pp. 619 – 625, 2015.
[17] H. T. Nguyen, Y. Han, M. Ernst, A. Fell, E. Franklin, and D. Macdonald, "Dislocations in laser-doped silicon detected by micro-photoluminescence spectroscopy," Appl. Phys. Lett., vol. 107, pp. 022101-1 - 022101-5, 2015.
[18] H. T. Nguyen, F. E. Rougieux, S. C. Baker-Finch, and D. Macdonald, "Impact of carrier profile and rear-side reflection on photoluminescence spectra in planar crystalline silicon wafers at different temperatures," IEEE Journal of Photovoltaics, vol. 5, pp. 77-81, 2015.